

# **An Asymptotic Preserving Scheme for Low Froude Number Shallow Flows**

**Koottungal Revi Arun and Sebastian Noelle**

**Bericht Nr. 352**

**Dezember 2012**

Key words: shallow water equations, low Froude number limit, stiffness, semi-implicit time discretisation, flux decomposition, asymptotic preserving schemes

Math. Subject Classifications : Primary: 35L65, 76B15, 76M45  
Secondary: 65M08, 65M06

**Institut für Geometrie und Praktische Mathematik  
RWTH Aachen**

**Templergraben 55, D-52056 Aachen (Germany)**

---

The first author is supported by the Alexander-von-Humboldt Foundation through a postdoctoral fellowship. The second author is partially supported by the Deutsche Forschungsgemeinschaft (DFG) under grant number NO 361/3-2.

## AN ASYMPTOTIC PRESERVING SCHEME FOR LOW FROUDE NUMBER SHALLOW FLOWS

K. R. ARUN AND S. NOELLE

Institut für Geometrie und Praktische Mathematik,  
RWTH-Aachen, Templergraben 55,  
D-52056 Aachen, Germany.

**ABSTRACT.** We present an asymptotic preserving (AP), large time-step scheme for the shallow water equations in the low Froude number limit. Based on a multiscale asymptotic expansion, the momentum fluxes are split into a nonstiff and a stiff part. A semi-implicit discretisation, where the nonstiff terms are treated explicitly and stiff terms implicitly in time, is crucial to achieve the AP property. A combination of the semi-discrete mass and momentum equations leads to an elliptic equation for the water height at the new time-level. With the aid of this, the momentum can be update explicitly using a large time-step which solely determined by the nonstiff characteristic speeds. The second order accuracy of the scheme is based on Runge-Kutta and Crank-Nicolson time-stepping procedures and MUSCL-type reconstructions. The numerical results clearly demonstrate the accuracy and robustness of the scheme and its efficacy to compute very low Froude number flows.

2010 *Mathematics Subject Classification* Primary 35L65, 76B15, 76M45; Secondary 65M08, 65M06

Shallow water equations, low Froude number limit, stiffness, semi-implicit time discretisation, flux decomposition, asymptotic preserving schemes

**1. Introduction.** In several problems of physics, engineering and industry, one often encounters processes acting on different spatial and temporal scales. In many situations, atmospheric and oceanic phenomena modelled by the shallow water equations are also reminiscent of such multiscale behaviours. In deep waters, e.g. where water-depth ranges up to 4000 metres, the speed of the gravitational waves on the ocean surface reaches up to 200 metres per second or more, while water moves only about 1-2 metres per second; see also [6]. In other words, there exists two different temporal (spatial) scales and in ocean dynamics such a disparity in the wave-speeds is usually quantified using the Froude number, which is the ratio of convection speed to gravitational wave-speed. A low Froude number flow is the shallow water analogue of the well known low Mach number hydrodynamics and hence it deserves a lot of attention from a mathematical point of view too. It has been rigorously proved, e.g. in [4], that the compressible Euler equations converge

---

2000 *Mathematics Subject Classification.* Primary: 35L65, 35L67, 35L40; Secondary: 65M06, 65M08, 76M25.

*Key words and phrases.* Shallow water equations, low Froude number limit, multiscale analysis, asymptotic preserving schemes.

The first author is supported by the Alexander-von-Humboldt Foundation through a postdoctoral fellowship. The second author is partially supported by the Deutsche Forschungsgemeinschaft (DFG) under grant number NO 361/3-2.

to their incompressible counter parts in the low Mach number limit. In fact, the low Mach number limit is a singular limit for the Euler system, therein the system of equations changes its nature from hyperbolic to mixed hyperbolic-elliptic.

We start with the shallow water system in the nondimensional form

$$\partial_t h + \nabla \cdot (h\mathbf{u}) = 0, \quad (1)$$

$$\partial_t(h\mathbf{u}) + \nabla \cdot (h\mathbf{u} \otimes \mathbf{u}) + \nabla \left( \frac{h^2}{2\varepsilon^2} \right) = 0, \quad (2)$$

where  $t \geq 0$  is time,  $\mathbf{x} \in \mathbb{R}^d, d = 1, 2$  is the space variable,  $h(\mathbf{x}, t) \geq 0$  is the water height,  $\mathbf{u}(\mathbf{x}, t) \in \mathbb{R}^d$  is the velocity vector. The operators  $\nabla, \nabla \cdot$  and  $\otimes$  are respectively the gradient, divergence and tensor products in  $\mathbb{R}^d$ .

Here, the nondimensional parameter  $\varepsilon := u_{\text{ref}}/\sqrt{gh_{\text{ref}}}$  is the reference Froude number which is the analogue of the Mach number in compressible flows. The asymptotic limit of the solutions to (1)-(2), as  $\varepsilon \rightarrow 0$ , can be investigated using the procedure due to Klainerman and Majda [4]. Formally, inserting the asymptotic ansatz

$$f(\mathbf{x}, t) = f^{(0)}(\mathbf{x}, t) + \varepsilon f^{(1)}(\mathbf{x}, t) + \varepsilon^2 f^{(2)}(\mathbf{x}, t) \quad (3)$$

for the unknown functions  $h$  and  $\mathbf{u}$  and equating the like powers of  $\varepsilon$  yields the limit equations

$$h(\mathbf{x}, t) = h^{(0)}(t) + \varepsilon^2 h^{(2)}(\mathbf{x}, t), \quad (4)$$

$$\nabla \cdot \mathbf{u}^{(0)} = -\frac{d}{dt} \log h^{(0)}, \quad (5)$$

$$\partial_t \left( h^{(0)} \mathbf{u}^{(0)} \right) + \nabla \cdot \left( h^{(0)} \mathbf{u}^{(0)} \otimes \mathbf{u}^{(0)} \right) + h^{(0)} \nabla h^{(2)} = 0. \quad (6)$$

Note that the water height  $h$  has two components: the spatially homogeneous leading order height  $h^{(0)}$  admits expansions or compressions at boundaries via the relation

$$\frac{1}{|\Omega|} \int_{\partial\Omega} \mathbf{u}^{(0)} \cdot \boldsymbol{\nu} \, d\sigma = -\frac{d}{dt} \log h^{(0)}, \quad (7)$$

while the second order height  $h^{(2)}$  serves the role of a Lagrange multiplier for the constraint (5).

The goal of the present work is to develop a numerical approximation to the shallow water system (1)-(2), in the context of the asymptotic preserving (AP) schemes [3], which is uniformly valid in  $\varepsilon$ . As  $\varepsilon \rightarrow 0$ , the standard explicit discretisations of (1)-(2) suffer from a severe restriction on the timestep due to the CFL condition, e.g. in one dimension

$$\text{CFL} := \frac{\Delta t}{\Delta x} \max_{\Omega} \left( |u| + \frac{\sqrt{h}}{\varepsilon} \right) \leq 1. \quad (8)$$

On the contrary, the AP schemes have the desirable property that their stability requirements are independent of the perturbation parameter  $\varepsilon$  and in addition they automatically detect the asymptotic limit (4)-(6) as  $\varepsilon \rightarrow 0$ . In other words, the limit of an AP scheme for (1)-(2) as  $\varepsilon \rightarrow 0$  is a consistent discretisation of the limit system (4)-(6).

Our design of a numerical scheme for the low Froude number flows is via a splitting of the flux functions in (1)-(2) into nonstiff and stiff parts based on the multiscale representation (4). The non-stiff parts of the fluxes are constructed in such a way that they have  $\mathcal{O}(1)$  eigenvalues when  $\varepsilon \rightarrow 0$ . Hence, in the discretisation

stage, the non-stiff part is treated explicitly in time, whereas the remaining stiff part is implicit in time. Following a crucial observation due to Degond and Tang [2], the elimination of implicit velocity terms leads to an elliptic equation for the water height, which complies with the divergence constraint (5) in the zero Froude number limit. Having solved the elliptic equation for the water height, the velocity can be computed explicitly. Hence, the scheme involves only two steps: the resolution of an elliptic equation and an explicit evaluation. The second order spatial accuracy of the scheme is achieved by using standard MUSCL type reconstructions, whereas the second order temporal accuracy is via Runge-Kutta midpoint predictions and Crank-Nicolson time stepping strategies.

**2. Asymptotic Preserving Time Discretisation.** Let  $0 = t^0 < t^1 < \dots < t^n < t^{n+1} < \dots$  be an increasing sequence of times and let  $\Delta t$  be the timestep at the  $n^{\text{th}}$  stage, i.e.  $t^{n+1} = t^n + \Delta t$ . We denote by  $f^n(\mathbf{x})$ , the approximation of any unknown function  $f$  at time  $t^n$ , i.e.  $f^n(\mathbf{x}) \sim f(\mathbf{x}, t^n)$ .

As a first step towards the construction of an AP scheme, as in [1, 5], we split the stiff pressure gradient term in (2) into nonstiff and stiff parts, i.e.

$$\nabla \left( \frac{h^2}{2\varepsilon^2} \right) = h\nabla h + \frac{(1-\varepsilon^2)}{\varepsilon^2} h\nabla h. \quad (9)$$

The AP time discretisation now consists of treating the second term on the right hand side of (9) and the mass flux implicitly, leading to the definition

**Definition 2.1.** The semi-implicit, semi-discrete, AP scheme is

$$h^{n+1} = h^n - \Delta t \nabla \cdot (h\mathbf{u})^{n+1}, \quad (10)$$

$$(h\mathbf{u})^{n+1} = (h\mathbf{u})^n - \Delta t \nabla \cdot (h\mathbf{u} \otimes \mathbf{u})^n - \Delta t h^n \nabla h^n - \Delta t \frac{(1-\varepsilon^2)}{\varepsilon^2} h^{n+1} \nabla h^{n+1}. \quad (11)$$

The details of the space discretisation and the fully discrete scheme will be presented later. In order to justify the above definition, we want to first show that the scheme (10)-(11) indeed possesses the AP property, i.e. as  $\varepsilon \rightarrow 0$ , it leads to a consistent discretisation of the limit system (4)-(6).

**Theorem 2.2.** *The semi-discrete, semi-implicit scheme (10)-(11) is AP.*

*Proof.* The proof of the AP property follows the same lines of asymptotic analysis in section 1. We propose the same three-term asymptotic ansatz

$$f^n(\mathbf{x}) = f^{n,(0)}(\mathbf{x}) + \varepsilon f^{n,(1)}(\mathbf{x}) + \varepsilon^2 f^{n,(2)}(\mathbf{x}) \quad (12)$$

for the discrete functions  $h^n$  and  $\mathbf{u}^n$ . Next, we balance the powers of  $\varepsilon$  on both sides of (10)-(11), e.g.  $\mathcal{O}(\varepsilon^{-2})$  and  $\mathcal{O}(\varepsilon^{-1})$  terms give

$$h^{n+1,(0)} \nabla h^{n+1,(0)} = 0, \quad (13)$$

$$h^{n+1,(0)} \nabla h^{n+1,(1)} + h^{n+1,(1)} \nabla h^{n+1,(0)} = 0. \quad (14)$$

Therefore, the leading order water height  $h^{n+1,(0)}$  and the first order water height  $h^{n+1,(1)}$  are spatially constants, yielding

$$h^{n+1}(\mathbf{x}) = h^{n+1,(0)} + \varepsilon^2 h^{n+1,(2)}(\mathbf{x}), \quad (15)$$

in consistency with (4). If we assume that the initial value of  $h$  also has the multi-scale representation (4), it then follows that (15) holds for all times.

Equating the  $\mathcal{O}(1)$  terms in (10)-(11) and using (15) gives

$$h^{n+1,(0)} = h^{n,(0)} - \Delta t \nabla \cdot (h\mathbf{u})^{n+1,(0)}, \quad (16)$$

$$(h\mathbf{u})^{n+1,(0)} = (h\mathbf{u})^{n,(0)} - \Delta t \nabla \cdot (h\mathbf{u} \otimes \mathbf{u})^{n,(0)} - \Delta t h^{n+1,(0)} \nabla h^{n+1,(2)}. \quad (17)$$

Note that (17) is clearly a consistent discretisation of (6), whereas in the light of (15), we can write (16) in the form

$$\nabla \cdot \mathbf{u}^{n+1,(0)} = -\frac{h^{n+1,(0)} - h^{n,(0)}}{h^{n+1,(0)} \Delta t}, \quad (18)$$

which is a consistent discretisation of the divergence constraint (5). Thus, the proof of AP property is complete.  $\square$

Our next step is to linearise the nonlinear term in (11). Before proceeding further, we would like to emphasise that we assume  $h > 0$  so as to avoid wet/dry areas. Let us denote  $\mathbf{q} = h\mathbf{u}$ , the momentum, we define an auxiliary height and momentum

$$\hat{h} := h^n - \Delta t \nabla \cdot \mathbf{q}^n, \quad (19)$$

$$\hat{\mathbf{q}} := \mathbf{q}^n - \Delta t \nabla \cdot \left( \frac{\mathbf{q} \otimes \mathbf{q}}{h} \right)^n - \Delta t h^n \nabla h^n. \quad (20)$$

The update formulae (10)-(11) can then be written in the form

$$h^{n+1} = h^n - \Delta t \nabla \cdot \mathbf{q}^{n+1}, \quad (21)$$

$$\mathbf{q}^{n+1} = \hat{\mathbf{q}} - \Delta t \frac{(1 - \varepsilon^2)}{\varepsilon^2} h^{n+1} \nabla h^{n+1}. \quad (22)$$

Using (22) in (21) leads to an elliptic equation

$$-\Delta t^2 \frac{(1 - \varepsilon^2)}{\varepsilon^2} \nabla \cdot (h^{n+1} \nabla h^{n+1}) + h^{n+1} = h^n - \Delta t \nabla \cdot \hat{\mathbf{q}} \quad (23)$$

for the water height  $h$ . In order to remove the nonlinearity of (23), we linearise the nonlinear term about the auxiliary height  $\hat{h}$  to get the linearised elliptic equation

$$-\Delta t^2 \frac{(1 - \varepsilon^2)}{\varepsilon^2} \nabla \cdot (\hat{h} \nabla h^{n+1}) + h^{n+1} = h^n - \Delta t \nabla \cdot \hat{\mathbf{q}}. \quad (24)$$

We solve the elliptic equation (24) to get the updated value of the water height  $h^{n+1}$ . The momentum update (22) can then be evaluated explicitly to get the velocity  $\mathbf{u}^{n+1}$ .

**3. Space Discretisation.** In this section, we present the details of the space discretisation and in order to make the exposition simpler, we restrict ourselves to the one-dimensional (1-D) case. However, the present ideas can be straight-forwardly extended to two space dimensions.

The split shallow water system can be written in the usual divergence form

$$\partial_t U + \partial_x \left( \hat{F}(U) + \tilde{F}(U) \right) = 0, \quad (25)$$

where

$$U = \begin{pmatrix} h \\ q \end{pmatrix}, \quad \hat{F}(U) = \begin{pmatrix} q \\ \frac{q^2}{h} + \frac{h^2}{2} \end{pmatrix}, \quad \tilde{F}(U) = \begin{pmatrix} 0 \\ \frac{(1 - \varepsilon^2)}{\varepsilon^2} \frac{h^2}{2} \end{pmatrix}. \quad (26)$$

As a first step in the numerical approximation, we discretise the given computational domain into uniform cells of size  $\Delta x$  and let  $C_i := \{x : |x - x_i| \leq \frac{\Delta x}{2}\}$  be the cell centred around the mesh point  $x_i = i\Delta x$ . The cell integral averages  $U_i^n$  are used

to approximate the solutions of the conservation law (25). Note that the semi-discrete formulation presented in the previous section requires the computation of the auxiliary height  $\hat{h}_i$  and the auxiliary momentum  $\hat{q}_i$ , for which we employ a finite volume update

$$\hat{U}_i = U_i^n - \frac{\Delta t}{\Delta x} \left\{ \hat{\mathcal{F}}_{i+\frac{1}{2}} - \hat{\mathcal{F}}_{i-\frac{1}{2}} \right\}. \quad (27)$$

Here, we use the Rusanov numerical flux

$$\hat{\mathcal{F}}_{i+\frac{1}{2}} = \frac{1}{2} \left( \hat{F}(U_i^n) + \hat{F}(U_{i+1}^n) \right) - \frac{a_{i+\frac{1}{2}}}{2} (U_{i+1}^n - U_i^n) \quad (28)$$

with

$$a_{i+\frac{1}{2}} := \max \left( |u_i| + \sqrt{h_i}, |u_{i+1}| + \sqrt{h_{i+1}} \right). \quad (29)$$

The elliptic equation (24) in the 1-D case reads

$$-\Delta t^2 \frac{(1-\varepsilon^2)}{\varepsilon^2} \partial_x \left( \hat{h} \partial_x h^{n+1} \right) + h^{n+1} = h^n - \Delta t \partial_x \hat{q}. \quad (30)$$

Employing central discretisations yields the linear system of equations

$$\begin{aligned} -\frac{\Delta t^2}{2\Delta x^2} \frac{(1-\varepsilon^2)}{\varepsilon^2} \left\{ \left( \hat{h}_{i+1} + \hat{h}_i \right) h_{i+1}^{n+1} - \left( \hat{h}_{i+1} + 2\hat{h}_i + \hat{h}_{i-1} \right) h_i^{n+1} \right. \\ \left. + \left( \hat{h}_i + \hat{h}_{i-1} \right) h_{i-1}^{n+1} \right\} + h_i^{n+1} = h_i^n - \frac{\Delta t}{2\Delta x} (\hat{q}_{i+1} - \hat{q}_{i-1}) \end{aligned} \quad (31)$$

We now show that our fully discrete scheme also possess the AP property.

**Theorem 3.1.** *The fully discrete scheme is AP.*

*Proof.* Let us consider the asymptotic expansion

$$f_i^n = f_i^{n,(0)} + \varepsilon f_i^{n,(1)} + \varepsilon^2 f_i^{n,(2)} \quad (32)$$

of the unknowns  $h_i^n$  and  $u_i^n$ . Next, we insert the ansatz (32) in (31) and equate to zero the like powers of  $\varepsilon$ . After using periodic boundary conditions,  $\mathcal{O}(\varepsilon^{-2})$  terms immediately gives  $h_i^{n+1,(0)} = \text{const} = h^{n+1,(0)}$ , say. In analogous manner we can obtain  $h_i^{n+1,(1)} = \text{const}$ . Hence,

$$h_i^{n+1} = h^{n+1,(0)} + \varepsilon^2 h_i^{n+1,(2)}. \quad (33)$$

In the light of (27) and after using (33), the leading order momentum update is

$$q_i^{n+1,(0)} = \hat{q}_i^{(0)} - \frac{\Delta t}{\Delta x} \hat{h}_i^{(0)} \left( h_{i+\frac{1}{2}}^{n+1,(2)} - h_{i-\frac{1}{2}}^{n+1,(2)} \right), \quad (34)$$

$$= q_i^{n,(0)} - \frac{\Delta t}{\Delta x} \left\{ \left( \frac{q^2}{h} \right)_{i+\frac{1}{2}}^{n,(0)} - \left( \frac{q^2}{h} \right)_{i-\frac{1}{2}}^{n,(0)} \right\} - \frac{\Delta t}{\Delta x} \hat{h}_i^{(0)} \left( h_{i+\frac{1}{2}}^{n+1,(2)} - h_{i-\frac{1}{2}}^{n+1,(2)} \right). \quad (35)$$

Note that (35) is clearly a consistent discretisation of the zero Froude number momentum conservation law (6). In order to obtain a discrete form of the mass conservation (5), we consider the  $\mathcal{O}(1)$  term in (31):

$$\begin{aligned} -\frac{\Delta t^2}{2\Delta x^2} \left\{ \left( \hat{h}_{i+1}^{(0)} + \hat{h}_i^{(0)} \right) h_{i+1}^{n+1,(2)} - \left( \hat{h}_{i+1}^{(0)} + 2\hat{h}_i^{(0)} + \hat{h}_{i-1}^{(0)} \right) h_i^{n+1,(2)} \right. \\ \left. + \left( \hat{h}_i^{(0)} + \hat{h}_{i-1}^{(0)} \right) h_{i-1}^{n+1,(2)} \right\} + h^{n+1,(0)} = h^{n,(0)} - \frac{\Delta t}{2\Delta x} \left( \hat{q}_{i+1}^{(0)} - \hat{q}_{i-1}^{(0)} \right) \end{aligned} \quad (36)$$

The quantity in the curly braces is a discretisation of  $\partial_x(\hat{h}^{(0)}\partial_x h^{n+1,(2)})$  and therefore, taking the difference form of (34) and comparing it with (36) we get

$$-\frac{\Delta t}{2\Delta x} \left( q_{i+1}^{n+1,(0)} - q_{i-1}^{n+1,(0)} \right) = h^{n+1,(0)} - h^{n,(0)}, \quad (37)$$

which can be rearranged to get a discrete version of (5). Hence, the proof of AP property is complete.  $\square$

**4. Second Order Extension.** The second order accuracy in time is achieved by the second order Runge-Kutta and Crank-Nicolson time stepping procedures, i.e.

$$U^{n+\frac{1}{2}} = U^n - \frac{\Delta t}{2} \partial_x \hat{F}(U^n) - \frac{\Delta t}{2} \partial_x \tilde{F}(U^{n+\frac{1}{2}}), \quad (38)$$

$$U^{n+1} = U^n - \Delta t \partial_x \hat{F}(U^{n+\frac{1}{2}}) - \frac{\Delta t}{2} \partial_x (\tilde{F}(U^n) + \tilde{F}(U^{n+1})). \quad (39)$$

The second order spatial accuracy is via standard MUSCL-type reconstructions and extrapolations.

**5. Numerical Case Studies.** In this section we report the results of some numerical experiments to assess the performance of our AP scheme. The capabilities of the AP scheme are more pronounced when its results are compared to those of a fully explicit scheme.

**5.1. Order of Convergence Under Grid Refinement.** Our first goal is to verify the convergence of our scheme and to this end, we consider an asymptotic solution

$$h(x, y, t) = 1 - \varepsilon^2 \{ \cos(4\pi(x-t)) + \cos(4\pi(y-t)) \}, \quad (40)$$

$$u(x, y, t) = 1 - 2 \cos(2\pi(x-t)) \sin(2\pi(y-t)), \quad (41)$$

$$v(x, y, t) = 1 + 2 \sin(2\pi(x-t)) \cos(2\pi(y-t)). \quad (42)$$

The asymptotic solution is constructed from an exact solution of the zero Froude number equations (4)-(6); see also [7] for more details. For at least a short time, the asymptotic solution will agree with an exact solution of the shallow water equations. Therefore, we initialise the variables with the asymptotic solution at  $t = 0$  and we do computations up to  $t = 0.01$ . We set  $\varepsilon = 0.005$  and divide the computational domain  $[0, 1] \times [0, 1]$  consecutively into  $20 \times 20, 40 \times 40, 80 \times 80, 160 \times 160$  cells. The boundary conditions are periodic everywhere. The  $L^1$  errors and the rates of convergence are in depicted table 1, which clearly demonstrate the second order convergence of the scheme.

$N$	$L^1$ error in $h$	Rate	$L^1$ error in $u$	Rate	$L^1$ error in $v$	Rate
20	0.00000939		0.00133667		0.00133667	
40	0.00000324	1.5340	0.00025461	2.3923	0.00025459	2.3924
80	0.00000049	2.7355	0.00005550	2.1978	0.00005551	2.1974
160	0.00000007	2.8878	0.00001227	2.1774	0.00001227	2.1780

TABLE 1. Errors and convergence computed using the asymptotic solution at  $t = 0.01$  and  $\varepsilon = 0.005$ .

**5.2. Two Colliding Pulses.** In this problem we model two colliding gravitational pulses in a 1-D channel. The motivation for this test is an analogous study reported in [5]. The initial data read

$$h(x, 0) = 0.955 + \frac{\varepsilon}{2} (1 - \cos(2\pi x)), \quad u(x, 0) = -\text{sign}(x)\sqrt{2} (1 - \cos(2\pi x)).$$

The computational domain  $[-1, 1]$  is divided into 200 equal mesh points and we have set  $\varepsilon = 0.1$ , the boundary conditions being periodic. The evolution of the water height at different times is shown in Figure 1.

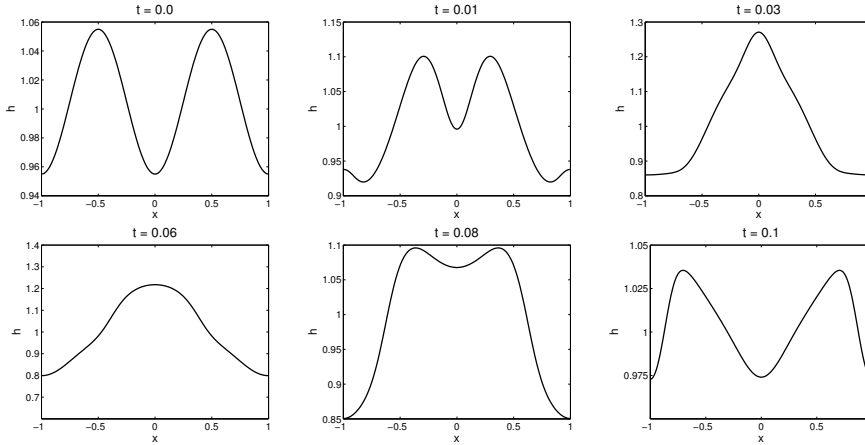


FIGURE 1. Two colliding gravitational pulses in a 1-D channel: evolution of water height at different times. Here,  $\varepsilon = 0.1$  and CFL number is 0.45.

**5.3. Advection of a Vortex.** In this test we simulate the advection of a vortex, which is a typical example of a low Froude number flow. Specifically, the initial data model a rotating vortex positioned at a point  $(0.5, 0.5)$  of the computational domain  $[0, 1] \times [0, 1]$  and superimposed in a uniform flow in the  $x$ -direction. The initial conditions are specified in terms of the radial distance  $r = \sqrt{(x - 0.5)^2 + (y - 0.5)^2}$  in the form

$$h(x, y, 0) = 0.5 + \varepsilon^2 h^{(2)}(r), \quad u(x, y, 0) = 1 - u_\phi(r) \sin \phi, \quad v(x, y, 0) = u_\phi(r) \cos \phi,$$

where

$$u_\phi(r) = \begin{cases} 5r, & \text{if } 0 \leq r \leq 0.2, \\ 2 - 5r, & \text{if } 0.2 \leq r \leq 0.4, \\ 0, & \text{otherwise.} \end{cases}$$

Here,  $\tan \phi = (y - 0.5)/(x - 0.5)$  and  $h^{(2)}$  satisfies  $\partial_r h^{(2)} = u_\phi^2/r$ . We have set  $\varepsilon = 0.001$  and the boundary conditions are periodic at left and right boundaries and wall on top and bottom. The computational domain is divided into  $160 \times 40$  mesh points. Figure 2 shows the isolines of the vorticity at times  $t = 0, 1, 2$  and 3.

In order to compare the dissipations of the AP scheme and a fully explicit scheme, we perform this experiment also for  $\varepsilon = 0.01$  and  $\varepsilon = 0.1$ . The relative kinetic energies obtained by both schemes are plotted in Figure 3. The figure clearly shows that the fully explicit scheme is far more dissipative than AP scheme and as  $\varepsilon$

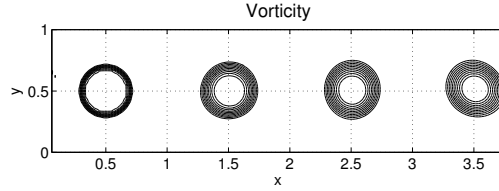


FIGURE 2. Advection of a vortex: isolines of the vorticity at times  $t = 0, 1, 2, 3$ , here  $\varepsilon = 0.001$ .

decreases, the dissipation of the explicit scheme decreases further. However, the dissipation of the AP scheme is almost independent of the Froude number  $\varepsilon$ .

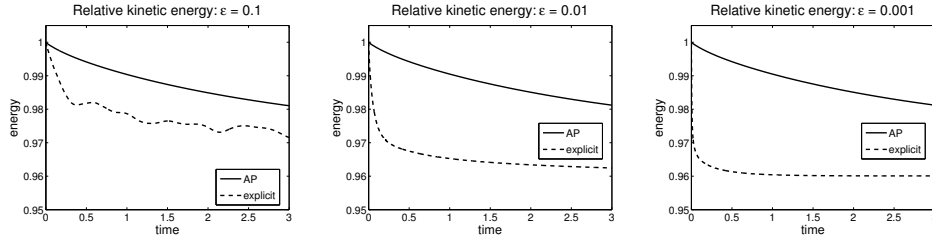


FIGURE 3. Advection of a vortex: relative kinetic energies for  $\varepsilon = 0.1, 0.01$  and  $0.001$ .

## REFERENCES

- [1] K. R. Arun, S. Nolle, M. Lukáčová-Medvičová, and C.-D. Munz. An asymptotic preserving all Mach number scheme for the Euler equations of gas dynamics. Technical Report 348, Institut für Geometrie und Praktische Mathematik, RWTH-Aachen, Germany, 2012.
- [2] P. Degond and M. Tang. All speed scheme for the low Mach number limit of the isentropic Euler equations. *Commun. Comput. Phys.*, 10(1):1–31, 2011.
- [3] S. Jin. Efficient asymptotic-preserving (AP) schemes for some multiscale kinetic equations. *SIAM J. Sci. Comput.*, 21(2):441–454, 1999.
- [4] S. Klainerman and A. Majda. Singular limits of quasilinear hyperbolic systems with large parameters and the incompressible limit of compressible fluids. *Comm. Pure Appl. Math.*, 34(4):481–524, 1981.
- [5] R. Klein. Semi-implicit extension of a Godunov-type scheme based on low Mach number asymptotics. I. One-dimensional flow. *J. Comput. Phys.*, 121(2):213–237, 1995.
- [6] O. Le Maître, J. Levin, M. Iskandarani, and O. M. Knio. A multiscale pressure splitting of the shallow-water equations. I. Formulation and 1D tests. *J. Comput. Phys.*, 166(1):116–151, 2001.
- [7] S. Vater and R. Klein. Stability of a Cartesian grid projection method for zero Froude number shallow water flows. *Numer. Math.*, 113(1):123–161, 2009.

Received xxxx 20xx; revised xxxx 20xx.

E-mail address: arun@igpm.rwth-aachen.de

E-mail address: noelle@igpm.rwth-aachen.de